

## **Chapter 4**

# **Microchannel flowed plasma process for micropatterning of myoblasts**

#### **4.1. Introduction**

The cellular organization is one of the primary steps involved in the structural formation of tissues and organs. The microenvironment of cells *in vivo* comprises extracellular matrix (ECM) and nearby cells, which help in essential processes, including cell proliferation, differentiation, migration, and apoptosis (Falconnet et al. 2006).

In the conventional scenario, the standard surfaces such as polystyrene dishes do not mimic the *in vivo* microenvironment as they offer rigid and flat substrate properties with no boundary conditions or cellular cues (Kapałczyńska et al. 2016). In order to mimic the *in vivo* microenvironment of skeletal muscle, various strategies have been applied, resulting in artificial skeletal muscle tissue models (Maleiner et al. 2018; Torii et al. 2018). One of the approaches that recapitulate the organised structure of skeletal muscle is micropatterning. Thus, the micro milieu created by micropatterning helps the cells to experience tissue like conditions *in-vitro* (Piel and Théry 2014; 2014; 2014). This process is convenient and highly effective in providing microenvironmental cues; thereby helps to study cellular mechanisms involving cell migration (M.C. Kim et al. 2013), cell polarization (Théry et al. 2006), differentiation (Bajaj et al. 2014), proliferation (Théry and Bornens 2006; Zatti et al. 2012), cell signaling (Kam, Shen, and Dustin 2013) and so on. Also, it permits fine tuning of the microenvironment influencing the cellular behavior in the desired manner (Thery 2010). Various methods of micropatterning applied for the purpose include microcontact printing (Gupta, Li, and Guo 2019), microfluidic patterning (Berry et al. 2017), stencil patterning (Rana, Timmer, and Neeves 2014; Shimizu, Fujita, and Nagamori 2010) and plasma lithography (Junkin, Leung, Yang, et al. 2011; Junkin, Leung, Whitman, et al. 2011; M.H. Lin et al. 2009). Usage of plasma lithography for patterning cells on polystyrene dishes and elastomeric substrates has been successfully demonstrated (Nam et al. 2015).

Furthermore, the creation of cellular micropatterns using plasma lithography and self-assembled monolayers (SAMs) of alkylsilane on a glass substrate is envisaged to serve as a potential platform for further exploration in cell biology. These tailored molecules of alkylsilanes help in modelling the cellular microenvironment to study the interactions of cells and extracellular matrix proteins at biointerfaces (Ostuni, Yan, and Whitesides 1999). In vitro, an interfacial layer of proteins or biomolecules present in the cell culture medium (serum components) helps mediate the cell adhesion onto the substrate/extracellular matrix. Cell adhesion is governed by a transmembrane cell surface receptor, i.e., integrin that aids in the formation of focal adhesion (FA) complex thus linking a substrate with the intracellular components (Nikkhah et al. 2012). Control is provided partly by interactions between transmembrane cell surface receptors and cell binding domains in the extracellular matrix. Upon contact with the microenvironment, there occur changes in the communication of cell adhesion; favorable on adhesive surfaces and detachment from the non-adhesive surfaces (Schwarz and Bischofs 2005). The communication allows for controlling the spatial distribution of cells that can be used to study various cellular functions (H. Zhang et al. 2016).

The chapter, reveals the use of microchannel flowed plasma process and alkylsilanes for micropatterning of glass substrates to create cell adhesive geometric constraint. The method overcomes problems of previous micropatterning processes like microcontact printing, micromolding in capillaries (MIMIC) and microfluidic patterning as it ensures fidelity of pattern transfer, multilength scale processing, and uniformity of pattern over large surfaces (M.H. Lin et al. 2009). PDMS stamps with varying microchannel features were used to obtain micropatterns with varying cell attachment widths, i.e., 20  $\mu\text{m}$ , 200  $\mu\text{m}$ , and 1000  $\mu\text{m}$ . The cell attachment widths used in the study are at a comparable length scale of myofiber diameter and muscle fascicle. The micropatterned surfaces were

characterized by conjugating with fluorescein isothiocyanate (FITC). To investigate the cell-substrate interactions, C2C12 myoblast cells were seeded on micropatterned substrates. The micropatterning technique creates stable patterns throughout in vitro culture and allows us to explore the effects of the geometric constraints on myoblast alignment in a time-dependent manner. Orientation order parameter (OOP) based analysis was used to interpret the interrelated impact of geometric constraint on the alignment of myoblasts. Furthermore, fluorescent actin staining and its orientation distribution analysis were done to study the influence of patterning on cell cytoskeleton. The development of micropatterned surfaces by the microchannel flowed plasma process helps to control the cellular alignment and responses of C2C12 mouse myoblasts. Furthermore, such control over the cells may provide an in-depth understanding of the process of in vitro myogenesis.

## **4.2. Materials and methods**

### **4.2.1. Materials**

Octadecyltrichlorosilane [Sigma Aldrich, Bengaluru, India], 3-aminopropyltriethoxysilane [Sigma Aldrich, Bengaluru, India], n-Hexane [SRL, Mumbai, India], Poly(dimethylsiloxane) [Dow Corning, Michigan, USA], Labolene [Thermo Fisher Scientific, Bengaluru, India], Acetone [SRL, Mumbai, India], Fluorescein 5(6)-isothiocyanate [Sigma Aldrich, Bengaluru, India], Dimethyl sulfoxide [Himedia, Mumbai, India], Dulbecco's modified Eagle's medium [Himedia, Mumbai, India], Fetal bovine serum [Himedia, Mumbai, India], Penicillin-streptomycin [Himedia, Mumbai, India], Bovine serum albumin [Himedia, Mumbai, India], Paraformaldehyde [Himedia, Mumbai, India], Triton x-100 [Himedia, Mumbai, India], Tetramethylrhodamine phalloidin [AAT Bioquest, Sunnyvale, California, USA] and 4',6-diamidino-2-phenylindole [Himedia, Mumbai, India].

#### 4.2.2. Patterning of hydrophilic and hydrophobic regions

Octadecyltrichlorosilane (OTS,  $\text{H}_3\text{C}(\text{CH}_2)_{17}\text{SiCl}_3$ ) and 3-aminopropyltriethoxysilane (APTES,  $\text{H}_2\text{N}(\text{CH}_2)_3\text{Si}(\text{OC}_2\text{H}_5)_3$ ) were purchased from Sigma Aldrich (product no-104817 and A3648, respectively). Glass coverslips were used to adsorb the monolayers of OTS, and APTES. Glass coverslips were cleaned with deionized water and 0.5% labolene. The surface of the glass coverslips was activated by air plasma [Electro-Technic Product, BD 20V Laboratory Corona treater, Chicago, USA] for 2 minutes on both sides. The activated coverslips were immersed in a solution of OTS/n-Hexane (1:10000 dilution) for 2 minutes. The coated coverslips were dried at room temperature. Finally, a complete monolayer of OTS was obtained on the glass substrates (Lin et al. 2009).

Thereafter, a polymeric mold made up of polydimethylsiloxane (PDMS) that served as a stamp was brought into conformal contact with the OTS coated coverslips. The plasma treatment was performed through the microchannels of the PDMS stamp. The plasma treatment modified the surface placed under the microchannels due to the formation of active oxygen species. There also occurred a localized modification of terminal functional groups from methyl to polar surface groups like hydroxyl, carboxyl, aldehyde, etc. The PDMS stamp was then removed from the coverslips carefully. The modified OTS/Si surface was further immersed in a solution of APTES/Acetone (1:10000 dilution) for 30 minutes. The locally modified OTS with terminal polar surface groups helped adsorption of APTES without interfering with the unmodified OTS maintaining the original surface characteristics (Figure 4.1).

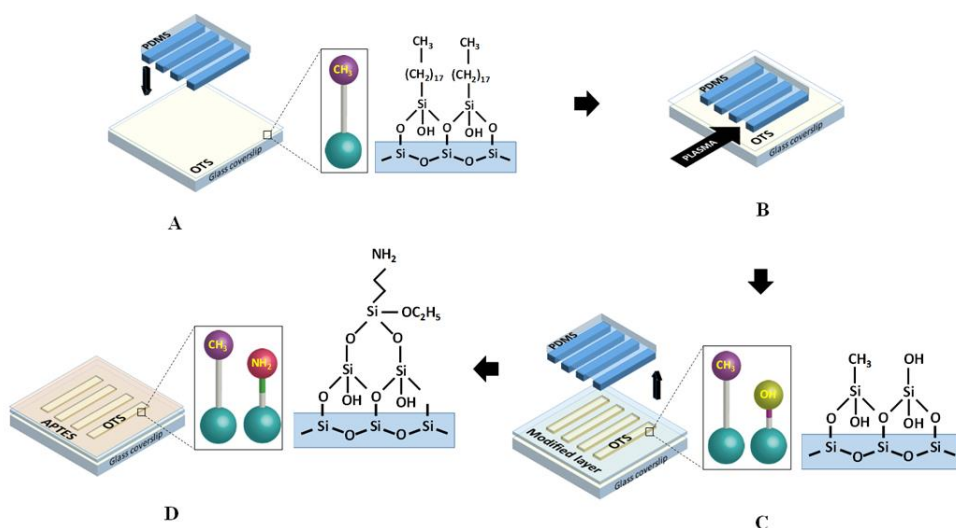


**Figure 4.1** Schematic illustration of micropatterning by selective surface modification of glass substrates. (A) Conformal contact of polydimethylsiloxane (PDMS) stamp on OTS modified glass coverslip with terminal  $-\text{CH}_3$  groups (B) Plasma treatment through the microchannels of PDMS stamps (C) Modification of surface terminal functional groups from  $-\text{CH}_3$  to polar groups like  $-\text{OH}$ ,  $-\text{CHO}$ ,  $-\text{COOH}$  (D) Grafting of APTES layer on the modified layer of OTS.

#### 4.2.3. Surface characterization of OTS/APTES coated glass coverslips

Fluorescein 5(6)-isothiocyanate (FITC) (product no - 46950) was used as an investigating tool for examining the modified surface, i.e., the coated OTS/APTES self-assembled monolayers. A stock solution of FITC (1mg/mL) was made in dimethyl sulfoxide (DMSO). The stock solution was subjected to vortex [Tarsons Spinix Vortex shaker, 3020] for 2 minutes for adequate mixing of FITC solution. A working solution of FITC in sterile PBS was prepared in the ratio of 1:50 (v/v) [Himedia, Mumbai, India]. The OTS/APTES coated coverslips were then immersed in the FITC/PBS solution for 2 h. The process of preparing a stock solution, working solution, and coating of FITC over OTS/APTES glass coverslips was performed in dark conditions. After FITC coating, the glass coverslips were washed with ethanol and deionized water. The coating of FITC over OTS/APTES was then visualized under an inverted fluorescence microscope (Nikon Ti-U Eclipse, Japan).

#### **4.2.4. Culture of C2C12 mouse myoblast cells on micropatterned substrates**

An immortalized myoblast cell, i.e., C2C12 was obtained from NCCS, India and was cultured in a T25 flask. The culture was supplemented with a medium consisting of Dulbecco's modified Eagle's medium (DMEM), 10% fetal bovine serum (FBS), and 1% penicillin-streptomycin. The cell suspension is maintained at 37 °C with a supply of 5% CO<sub>2</sub>. The cells were trypsinized and seeded on micropatterned surfaces. Media was changed every two days.

#### **4.2.5. Orientation order parameter calculation to understand alignment on micropatterned surfaces**

The degree of alignment observed within the cells was quantified using a metric orientation order parameter (OOP) which is generally used in evaluating the orientations of two-dimensional liquid crystals (Umeno et al. 2001; Umeno and Ueno 2003; Sun, Tang, and Ding 2009). For the calculation of the parameter, the angle made by the axis of each cell with the direction of micropatterning (i.e., vertical direction) was measured using Image J software. The angular measurements were made on images acquired from three separate individual experiments for each of the micropatterns. Further, the orientation order parameter was calculated using the formula  $OOP = 2(\langle \cos^2\theta \rangle - 0.5)$ . The OOP values range from 0 for entirely unaligned cells to 1 for wholly aligned cells. Statistical analysis was performed by using one-way ANOVA post hoc Tukey means of comparison. The values obtained were represented as mean  $\pm$  standard deviation.

#### **4.2.6. Fluorescent staining of actin and nuclei on micropatterned surfaces and actin-orientation distribution analysis**

Fluorescent staining of C2C12 cells on various micropatterned cell adhesive widths viz, 20  $\mu$ m, 200  $\mu$ m, and 1000  $\mu$ m was performed; briefly, the cells were fixed for 20 minutes in 4% paraformaldehyde. Followed by permeabilization in 0.1% triton x-100 for 10 minutes and blocking in 1% bovine serum albumin (BSA) for 30 minutes. For actin staining the blocked cells were subjected to Tetramethylrhodamine phalloidin (1X

concentration) for 1 h. Finally, the cells were visualized under an inverted fluorescence microscope [Nikon Ti-U Eclipse, Japan] after staining with 4',6-diamidino-2-phenylindole (DAPI) for 30 minutes. All the procedures were performed at room temperature.

The actin-stained fluorescent images of micropatterned C2C12 cells are converted into 8-bit grey scale image using Fiji (Schindelin et al. 2012). The micropatterned pattern is selected using a rectangular region of interest and is further subjected to Orientation J plugin to obtain a plot of distribution of orientation vs orientation in degrees (Rezakhaniha et al. 2012).

### **4.3. Results and discussion**

#### **4.3.1. Surface Analysis of FITC-APTES bonding over the glass substrates**

In order to characterize the OTS/APTES micropatterned substrates, a FITC-APTES bonding was used. The technique involves incubation of FITC with micropatterned glass substrates followed by efficient washing; resulting in low noise from the background field of view under a fluorescence microscope. The reactive isothiocyanate groups readily bind to the terminal amine groups of APTES, whereas it lacks reactivity with the methyl-terminated groups of OTS. Figure 4.2 shows the FITC based surface characterization of adhesive regions having a width of 20  $\mu\text{m}$ , 200  $\mu\text{m}$ , and 1000  $\mu\text{m}$ .

The fluorescence images thus reveal that the adopted process for micropatterning can effectively create cell adhesive widths of APTES, which have dimensions comparable to the diameter of the myofiber. The adhesive regions are ready to be seeded with cells i.e., C2C12 myoblasts cells. The surface characterization of OTS/FITC coated glass coverslips revealed the complete coating of cell adhesive regions. The fluorescence imaging of the FITC bound to the primary amine groups of APTES shows the uniform



coating of the adhesive layer on the glass coverslips while methyl terminated OTS groups show no bonding to FITC.

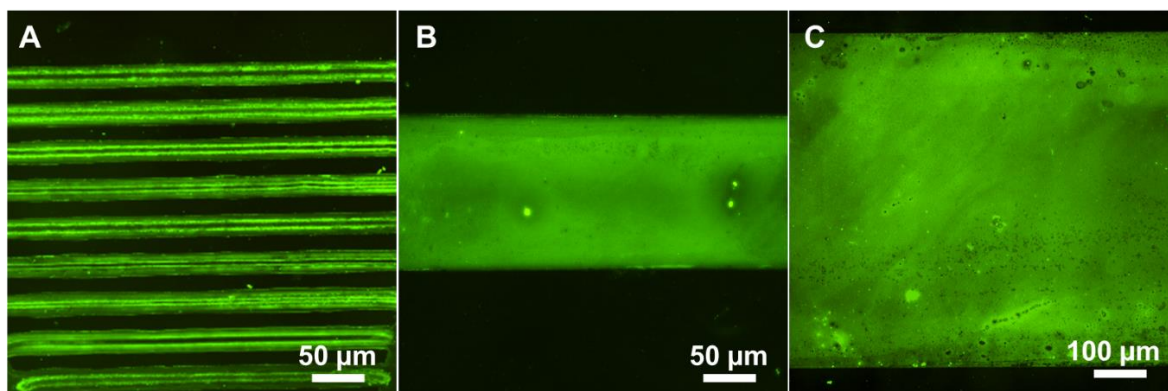


**Figure 4.2** Surface characterisation of OTS/APTES coated glass coverslips using FITC showing micropatterns of different widths: (A) 20 µm (B) 200 µm (C) 1000 µm.

#### 4.3.2. Alignment of C2C12 myoblast cells

In order to observe the alignment of myoblasts on micropatterned glass substrates in a temporal manner, bright field microscopy was performed. The bright-field microscopic images show C2C12 mouse myoblast cells cultured on OTS/APTES modified glass coverslips having variable widths of cell adhesive regions, i.e., 20 µm, 200 µm, and 1000 µm. Figure 4.3, 4.4, and 4.5 represent bright field images of C2C12 myoblast culture after 2 days, 5 days and 8 days on different widths of 20, 200 and 1000 µm respectively. Representative images clearly show myoblasts aligning themselves to adhesive regions. Moreover, the change in surface chemistry is aiding the cell attachment on cell adhesive regions.

The initial adhesion of cell followed by alignment on micropatterned surfaces suggests the positive influence of terminal amine groups provided by hydrophilic APTES. The adherence of biological materials (cell, tissues) has been widely regulated with various terminal functional groups such as an amine (-NH<sub>2</sub>), hydroxyl (-OH), carboxyl (-COOH), methyl (-CH<sub>3</sub>) and polyethylene glycol (PEG). Previous reports have revealed that the growth of cells is notably more on SAMs terminated with amine groups than on carboxyl

groups and least on methyl, hydroxyl, and PEG (Faucheux et al. 2004). Also, methyl-terminated SAMs are observed to inhibit cellular adhesion leading to G1 arrest in the process of the cell cycle (J. Li et al. 2015). Similarly, the microscopic images showed that some of the cells that were attached to non-adhesive regions got detached and began to die after subsequent days of culture. Throughout the culture after 5 days and 8 days, it shows that C2C12 myoblast cells are aligned and are found well within the cell-adhesive regions. It is of particular interest that although the width of cell-adhesive areas decreases from 1000  $\mu\text{m}$  to 20  $\mu\text{m}$ , the alignment is quite evident (Day 2 images of C2C12).

Moreover, observation in the broader regions reveals the likelihood of cellular alignment at first near the boundaries or at the interface of hydrophobic and hydrophilic regions and subsequent alignment of all the cells with the progression of culture (Figure 4.5). Previous studies have described the cell dynamics in culture especially for the cells present at the interface or near the boundary region of the micropatterned surface (i.e., cell-adhesive areas) (Junkin, Leung, Whitman, et al. 2011; Rolli et al. 2012). Notably, the work by Rolli et al. reports the classification of the cells observed at such interface into leader and follower cells.

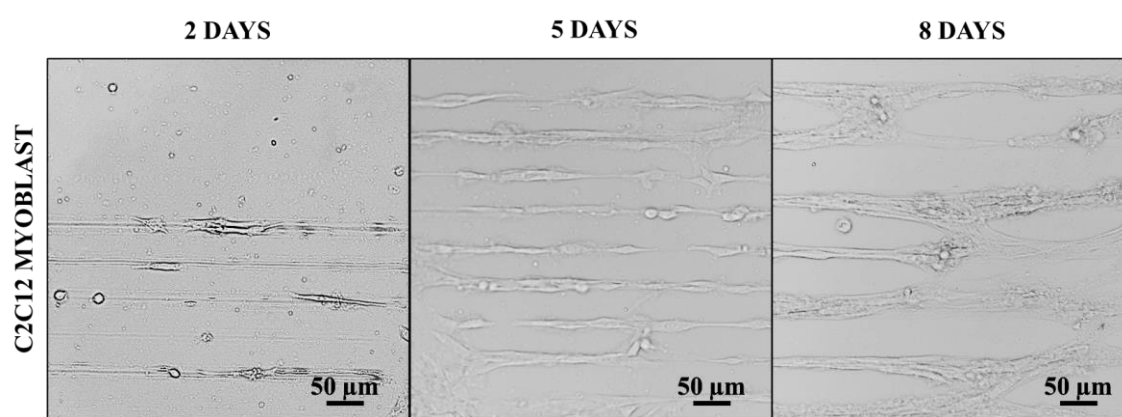


**Figure 4.3** Bright-field images of C2C12 skeletal myoblast cells cultured on cell adhesive width of 20  $\mu\text{m}$  for 2, 5, and 8 days.

Another study has revealed the importance of left-right asymmetry surrounding the cells through micropatterning, suggesting its critical role in the development of tissue (Wan et

al. 2011). Similar observations were noticed undoubtedly in our culture as well, in particular, in cell-adhesive regions having a width of 200  $\mu\text{m}$  and 1000  $\mu\text{m}$  (Figure 4.4 and 4.5).

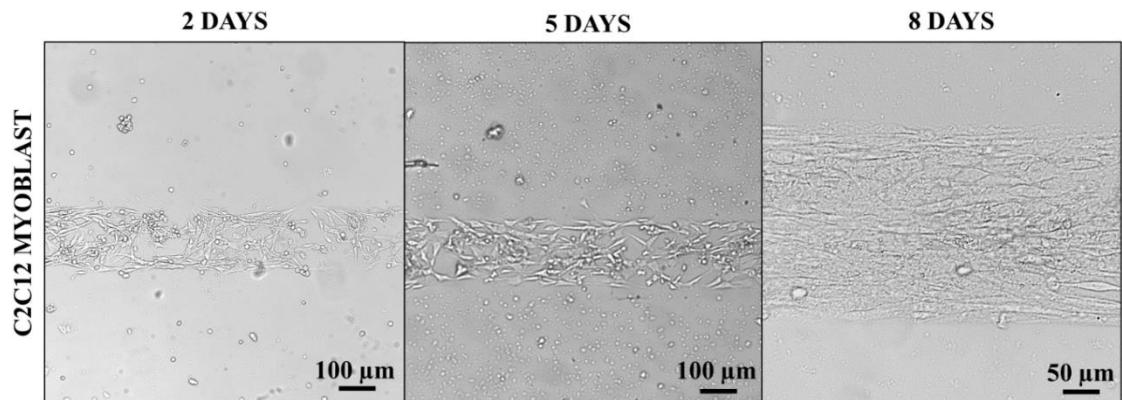


**Figure 4.4** Bright-field images of C2C12 skeletal myoblast cells cultured on cell adhesive width of 200  $\mu\text{m}$  for 2, 5, and 8 days.

The cells at the interface were found aligned themselves to cell-adhesive cues most likely provided by the terminal functional groups of SAM; whereas cells away from the interface and located in the inner zone of cell adhesive regions were noticeably adhered and elongated randomly.

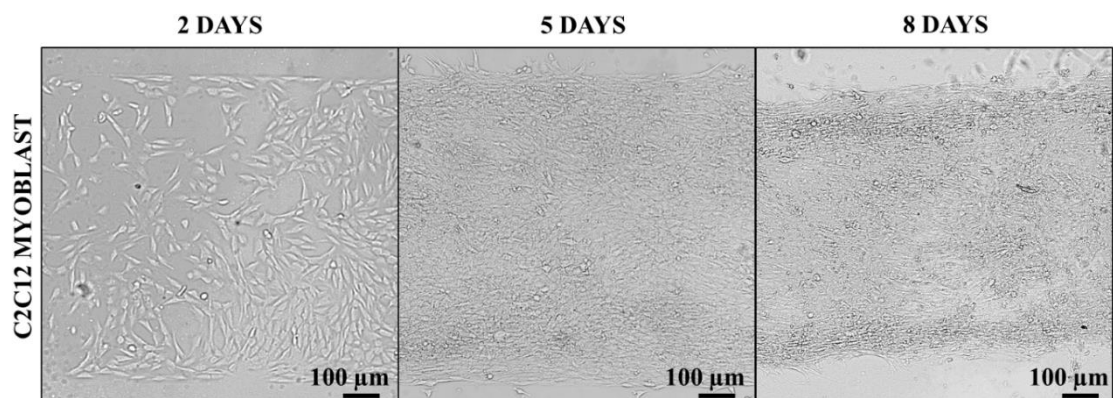


**Figure 4.5** Bright-field images of C2C12 skeletal myoblast cells cultured on cell adhesive width of 1000  $\mu\text{m}$  for 2, 5 and 8 days.

It is evident from the above reports that information received by the cells at the interface leads to their alignment first, and then they communicate to the neighbouring cells for a similar arrangement. This cell-cell communication further propagates and gets

transmitted to cells even placed in the middle of the cell-adhesive regions (Nava, Raimondi, and Pietrabissa 2014).

### 4.3.3. Orientation order parameter analysis supports the gradual alignment of myoblasts

In order to further characterize the alignment of myoblasts observed on micropatterned substrates, an OOP based approach was applied (Umeno and Ueno 2003; Sun, Tang, and Ding 2009). The orientation order parameter values calculated from the bright field images of C2C12 skeletal myoblast cells cultured on the micropatterned surfaces at days 2, 5, and 8, respectively, are represented in Figures 4.6.

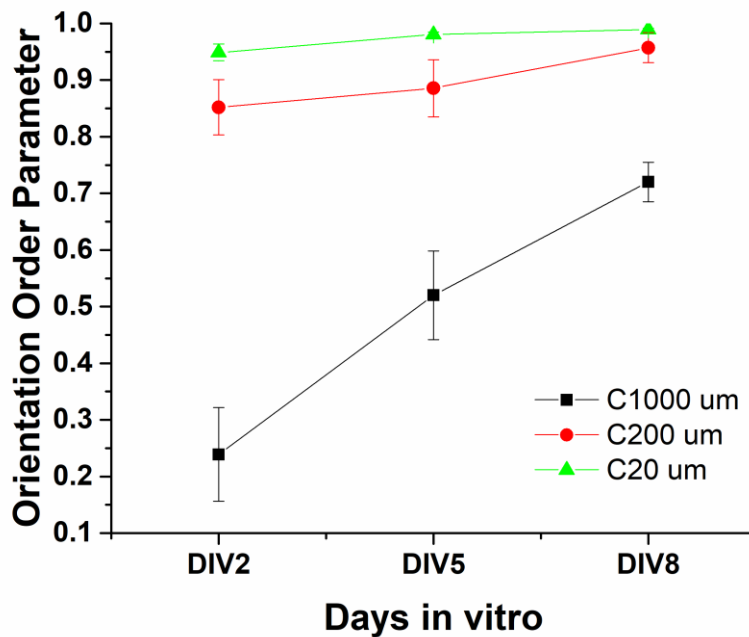


**Figure 4.6** Graph showing the orientation order parameter of C2C12 myoblasts and primary skeletal muscle cells cultured on cell adhesive widths of 20  $\mu\text{m}$ , 200  $\mu\text{m}$  and 1000  $\mu\text{m}$  respectively on 2, 5 and 8 days respectively. Symbols for C20, C200 and C1000 denote C2C12 cell cultured on micropattern widths of 20  $\mu\text{m}$ , 200  $\mu\text{m}$  and 1000  $\mu\text{m}$  respectively.

In Figure 4.6, it can be seen that as soon as the C2C12 cells are seeded on 20  $\mu\text{m}$  adhesive width, it can be observed that the cells are aligned within a period of 2 days from seeding. The cellular alignment further improves to a minor extent to achieve a near to perfect

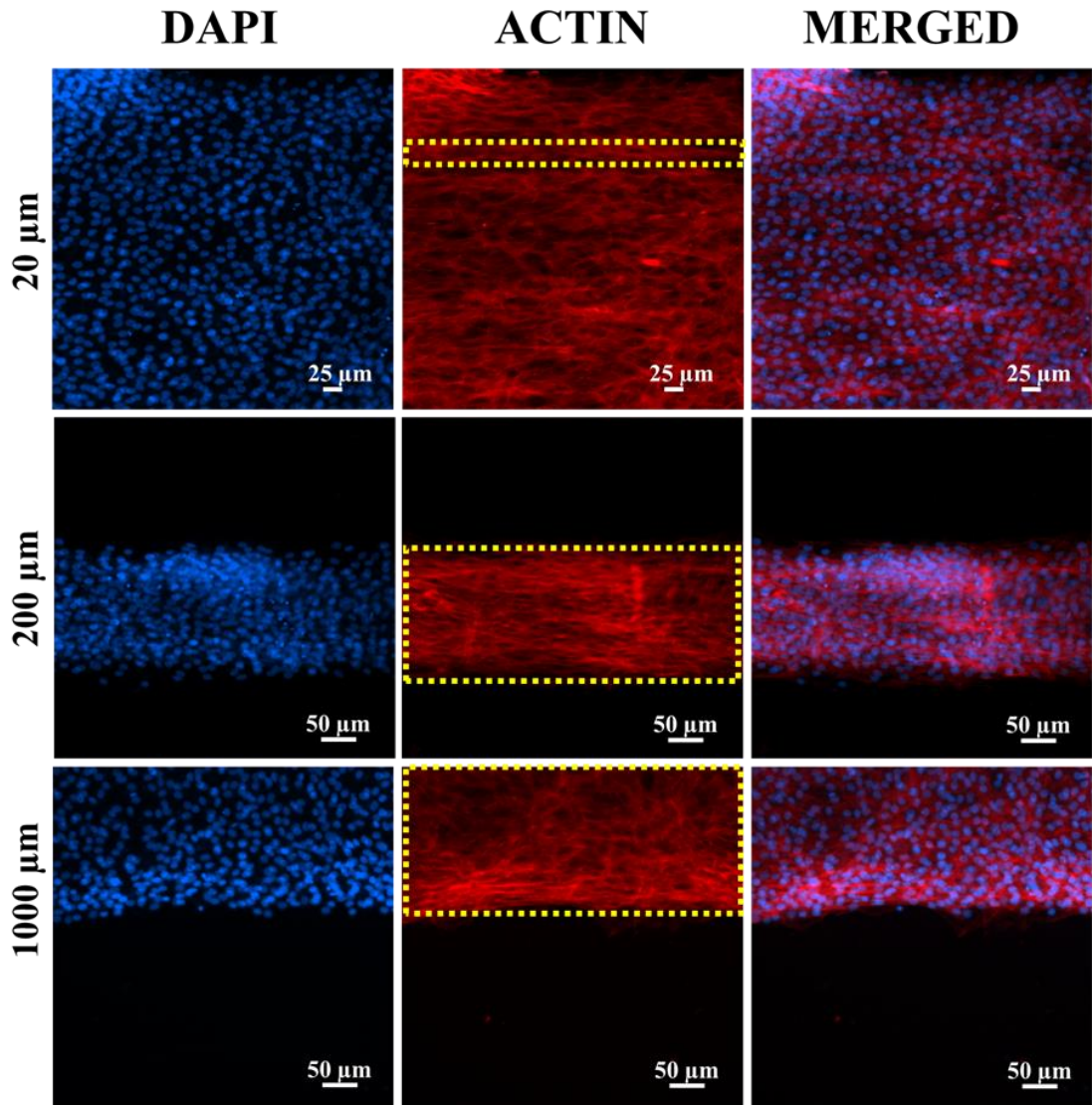
alignment owing to OOP values attaining very close to one. A similar sort of observation is made concerning C2C12 cells on 200  $\mu\text{m}$  micropatterned adhesive width, the cells show OOP values near to 1, and the OOP values remain nearly stable with increase culture duration. The OOP curve corresponding to C2C12 cells on 1000  $\mu\text{m}$  pattern shows low OOP value corresponding to day 2 in comparison to the other micropatterns. The OOP values further increase significantly at 5th day of culture and maintain the values near to 0.7 in 8 days.

Overall, the cells attain good alignment on the 8<sup>th</sup> day of in vitro culture. A significant amount of alignment of cells is observed for the cells patterned on 1000  $\mu\text{m}$  pattern (significant at the level  $p=0.01$ ) during the culture period. On day 2, it can be observed that the cells have adhered and aligned on all the micropatterns except for the case of 1000  $\mu\text{m}$  pattern wherein the cells show significantly lower OOP compared to 20 and 200  $\mu\text{m}$  pattern (0.001 level of significance).

OOP based analysis of the myoblasts leads to an observation that the alignment of the cells was directly dependent upon the area of geometric confinement or initial cell adhesion width of the micropattern. Thus, an early alignment in 20  $\mu\text{m}$  and 200  $\mu\text{m}$  micropatterns was observed, which is evident by OOP value on day 2. There was a difference in OOP value for 1000  $\mu\text{m}$  micropatterns may be due to the availability of larger surface area for the adherence of cells. C2C12 cells show similar OOP values on the 5<sup>th</sup> and 8<sup>th</sup> day for each of the micropatterns used in the study indicating the alignment of cells irrespective of the micropattern. The temporal variation in OOP values in the cells with 200 $\mu\text{m}$  and 1000  $\mu\text{m}$  pattern suggests that the cellular alignment may have proceeded from boundary to the center of the pattern with culture duration (Bajaj et al. 2014; Zatti et al. 2012; Junkin, Leung, Whitman, et al. 2011).

#### **4.3.4. Cytoskeletal actin staining and its orientation in micropatterned substrates**

In order to understand the effect of micropatterning on the actin cytoskeleton and nuclei, fluorescent staining of the C2C12 cells was performed on the micropatterned substrates after 8 days of culture. Figure 4.7 represents the results of fluorescent staining of actin/nuclei and results of actin orientation distribution on each of the micropatterned substrates of 20  $\mu\text{m}$ , 200  $\mu\text{m}$  and 1000  $\mu\text{m}$  respectively (moving from top to bottom). For each of the patterns (moving from left to right) the left most image represents the DAPI stained nuclei, center image panel represents the rhodamine-phalloidin stained actin cytoskeleton and the third image across the horizontal represents the merged image of both the images. Actin-stained images were analyzed for their distribution of orientation using an Image J plugin, Orientation J (Rezakhaniha et al. 2012; Rueden et al. 2017). The yellow rectangular region of interest indicated in each of the actin-stained images was used for the analysis. The results of orientation distribution analysis for each of the micropattern are represented in the right most panel of Figure 4.7. The graph of actin orientation distribution shows angle of orientation on the x-axis ranging between  $-90^\circ$  to  $+90^\circ$  and normalized orientation distribution of actin along y-axis. In addition to the orientation order parameter analysis of myoblasts, fluorescence staining of C2C12 cells on micropatterned widths with respect to their actin cytoskeleton and nuclei was carried out. Actin plays a significant role in the dynamics of myoblasts involving attainment of a characteristic bipolar morphology. Reorganization of actin and non-muscle myosin 2A and their interactions lead to localisation of focal adhesions at the ends of the myoblasts resulting in a bipolar morphology. Such a bipolar morphology allows them to form aligned myoblast groups. Formation of such organised myoblast groups is one of the essential prerequisites before myoblast fusion process (Peckham 2008).



### ACTIN ORIENTATION DISTRIBUTION

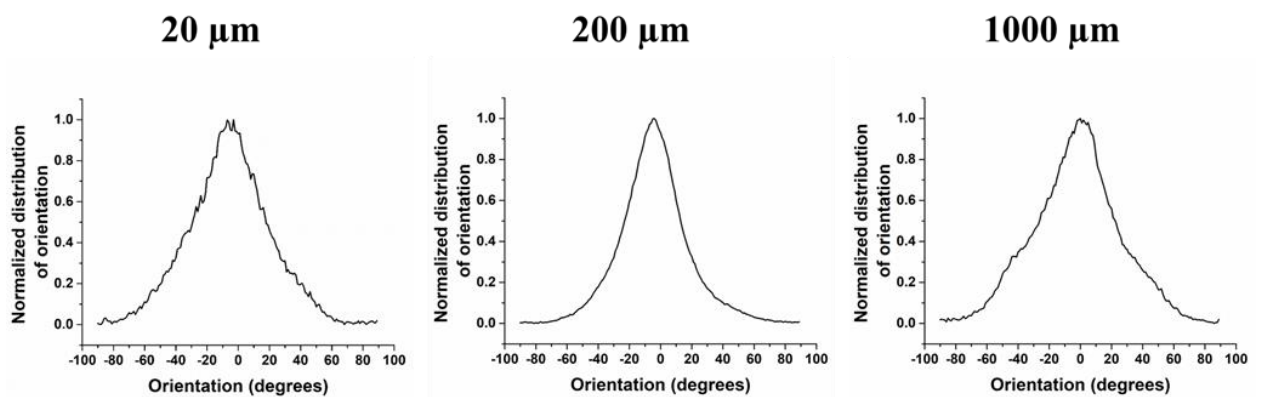


**Figure 4.7** Fluorescence images of micropatterned C2C12 cells stained with DAPI (nuclei), Rhodamine phalloidin (actin) and merged images along with the graph of actin orientation distribution analysis in the bottom (moving from left to right) on different cell adhesive widths of 20  $\mu\text{m}$ , 200  $\mu\text{m}$  and 1000  $\mu\text{m}$  (moving from top to bottom) respectively. The region of interest indicated in the actin image denotes the area used for orientation distribution analysis.

The remodeling of actin plays a significant role in normal functioning of skeletal muscle tissue. Pharmacological inhibition of actin remodeling in vitro culture results in negative implications with respect to differentiation and fusion of myoblasts (Nowak et al. 2009). In Figure 4.7, it can be observed that, for 20  $\mu\text{m}$  pattern the C2C12 myoblasts have attained a highly aligned morphology with respect to their actin cytoskeleton and nuclei owing to the limited area of cell adhesion as shown in the fluorescence images for actin as well as the merged images of actin and nuclei. Further, analysis of actin orientation distribution was done by setting the orientation parallel to micropattern to be equal to zero degrees. The orientation distribution analysis in 20  $\mu\text{m}$  pattern reveals that majority of the cells are oriented with an angle of 3-7° degrees in deviation to the horizontal direction (which is considered as zero degrees). This deviation lies within the 15 degrees value under which the cells are considered to be aligned (Bajaj et al. 2011). Thus, leading to a conclusion that the actin cytoskeleton in the cells have aligned to the 20  $\mu\text{m}$  pattern after 8 days of in vitro culture. In the case of 200  $\mu\text{m}$  pattern, it can be found that the C2C12 cells after 8 days in vitro also showed a highly aligned actin cytoskeleton along with their corresponding nuclei. The near perfect alignment of actin cytoskeleton of the cells present at the boundary of cell adhesive width can be clearly seen in the images corresponding to the pattern. Actin orientation distribution analysis of the 200  $\mu\text{m}$  pattern reconfirms the observations from the actin- stained image with majority of the actin are oriented in the angle of 4-5° degrees with respect to horizontal direction.

Similarly, the fluorescent images corresponding to 1000  $\mu\text{m}$  pattern show an aligned nature of actin cytoskeleton along the peripheral regions of the cell adhesive widths which deviates to a good extent by moving from peripheral region to the interior of the pattern in a direction perpendicular to the horizontally shown image. The orientation distribution analysis of the actin-stained image shows that the actin orientations lie within a slightly



broader range of angle deviations. It can be observed that the actin orientations are divided at three angles  $+45^\circ$ ,  $-45^\circ$  and primary angle of orientation near to  $0^\circ$  with respect to the horizontal direction. Such a broad range of actin orientation distribution may be due to the larger area of cell adhesion. Probably, in  $1000\ \mu\text{m}$  width the cells are in a transition phase where in on further in vitro culture they may transmit alignment information leading to a single peak in actin orientation analysis as well as OOP value close to one. In addition, owing to the limited cell adhesive area in  $20\ \mu\text{m}$  and  $200\ \mu\text{m}$  widths the alignment has completed by 8 days of culture. Overall, the actin fluorescent staining along with orientation distribution analysis discloses some essential observations. Firstly, the attainment of bipolar morphology by C2C12 myoblasts at the peripheral boundary regions of micropatterns. Actin-orientation distribution analysis suggests an overall alignment of actin in C2C12 cells across all the micropatterns. These observations are in coherence with the results of OOP analysis in micropatterned C2C12 cells.

In vivo, cells are surrounded by neighboring cells and structured microenvironment as extracellular matrix (ECM). The ECM provides an environment for cellular signaling molecules and serves as mechanical support. It comprises tissue-specific structural proteins such as collagen, fibronectin, laminin, vitronectin, elastin, and glycosaminoglycan (GAG) network. Collagen and elastin provide mechanical resistance to shear and tensile stress, whereas GAGs offer compressive strength to tissues due to the presence of hydrophilic groups (Frantz, Stewart, and Weaver 2010). The interaction of cells (1) with ECM containing different binding sites is regulated by the specific receptor known as integrin and (2) with neighboring cells through another receptor known as cadherins. The cell interaction with its specific microenvironment activates cell transduction pathways which are instrumental in the observation of cell dynamics, behavior and fate of the cell (Nava, Raimondi, and Pietrabissa 2012). This can be

influenced by biochemical cues presented by chemical modification of the surface of the substrate for example through creating anchorage monomers similar to ECM binding sites or by facilitating terminal functional groups such as hydroxyl, amine, thiol and carboxylic groups (J. Li et al. 2015). However, the process of cell adhesion to a material with particular engineering properties such as microgeometry, stiffness, nanotopography and surface modification triggers the generation of a variable degree of cytoskeletal tension within the cells. This occurs because of the complex system of intracellular components and signal transduction cascades that result in the production of traction forces and subsequent changes in cellular behavior. In the case of adhesion mediated traction forces, the cytoskeletal tensions are primarily balanced by actomyosin contractility and extracellular forces provided by the substrate (Bershadsky, Balaban, and Geiger 2003). Therefore, when there is a variation in the adhesion mediated traction forces across the intracellular regime of a cell, there occurs anisotropic cytoskeletal tension, and the cell appears to be elongated. In contrast, the roundish shape of the cell is generally observed when there is relatively no or little variation in adhesion mediated traction forces. The traction forces are sensed by the transmembrane receptors like integrins which transmit mechanical signals to intra cellular space. The actin present within the myocytes align themselves according to the externally applied mechanical tension and more focal adhesion complexes are recruited at high tension regions of myocytes which are again connected with newly polymerised actin fibers. Such external mechanical signals are further converted into biochemical signals which alter gene expression in myocytes (Bray, Sheehy, and Parker 2008; Geisse, Sheehy, and Parker 2009). The organized alignment of the actin is as a result of the mechanical tension experienced by the myocytes. Inhibition of actin is achieved by using drugs like Latrunculin A, Cytochalasin D and Jasplakinolide. A higher concentration of actin inhibiting drugs effects the survival

of the cells. Application of such drugs at lower concentration altered the boundary induced biased migration of circularly micropatterned C2C12 cells (Wan et al. 2011). Furthermore, inhibition of actin in mesenchymal cells changes the cell morphology from spindle shape to round morphology, this is due to the either a breakage of actin filaments or their irregular organisation (Müller et al. 2013).

In this study, the bipolar morphology of myoblasts adhered at the interface of hydrophobic and hydrophilic regions thus suggests the likelihood of varying levels of traction forces across the cellular regimes resulting from the change in ECM cues at the interface. Further, the cell cues possibly propagate from the cells adhered and aligned at the interface to the cells adhered towards the central portion of the adhesive width; resulting in the alignment of both categories of cells, i.e., located at the interface and inside the adhesive width to be in the same direction (Nava, Raimondi, and Pietrabissa 2014; 2012). This is also supported by the OOP analysis of the myoblasts. Such an observation of myoblast-myoblast physical interaction and communication of alignment orientation across the micropatterned widths of 1 mm was reported by Junkin and co-workers. The study also observed that such transmission of alignment information occurs only in differentiated myoblasts and not in other cells (Junkin, Leung, Whitman, et al. 2011).

Further, the fluorescent staining of actin followed by orientation distribution analysis also reemphasises the influence of micropatterning on the cytoskeleton alignment of the myoblasts. The analysis also supports the transfer of alignment information across the cell adhesive width. Hence, this simple technique of micropatterning involving plasma and alkylsilanes could be used in the exploration and understanding of the processes concerning to alignment of myoblasts.

Thus, cellular mechanisms like cell polarization, migration, proliferation and differentiation have been explored by various micropatterning methods like microcontact printing (Gupta, Li, and Guo 2019), microfluidic patterning (Berry et al. 2017), stencil patterning (Rana, Timmer, and Neeves 2014; Shimizu, Fujita, and Nagamori 2010) and plasma lithography (Junkin, Leung, Yang, et al. 2011; Junkin, Leung, Whitman, et al. 2011). In this study, microchannel flowed plasma process and alkylsilanes for micropatterning of glass substrates to create cell adhesive geometric constraint. The method overcomes problems of previous micropatterning processes like microcontact printing, micromolding in capillaries (MIMIC) and microfluidic patterning as it ensures fidelity of pattern transfer, multilength scale processing, and uniformity of pattern over large surfaces (M.H. Lin et al. 2009). To the best of my knowledge the microchannel flowed plasma process has been applied for the first time to create and assess the physiologically relevant micropatterns that are useful for studying the alignment process of C2C12 mouse myoblast cells. Further, the analysis of alignment was carried out by application of orientation order parameter and orientation of cytoskeletal actin.

The microchannel flowed plasma process of micropatterning explored in this chapter has utilized in chapter 6 to understand the influence of substrate micropatterning on primary satellite cells isolated from rat hind limb skeletal muscle cells. For this purpose, skeletal muscle cells were cultured and characterized for a period of 14 days on micropatterned glass substrates. Several characteristic parameters of muscle differentiation, including the fusion index, maturation index, and average width of the myotubes were quantified. The functional behavior of cultured myotubes exhibiting spontaneous contractions was assessed through kymograph to determine the twitch frequency. In addition, the degree of alignment of myotubes was evaluated on micropatterned substrates through examining orientation order parameter and two-dimensional fast Fourier transform analysis.

#### **4.4. Summary**

The chapter successfully applied the microchannel flowed plasma process for creating micropatterns using alkyl silanes OTS/APTES on glass substrates. The method was used to develop the cell-adhesive regions having widths of 20, 200, and 1000  $\mu\text{m}$ . Using FITC based conjugation; confirmed the formation of micropatterns on the glass substrates. The micropatterned glass substrates were used to culture C2C12 myoblast cells. This study corroborates the alignment of the myoblasts using surface cues facilitated by changing surface chemistry of the glass substrates. The outcomes of OOP analysis support the microscopic observations; indicating that the alignment of myoblasts may have started initially at the boundary of the micropatterns due to the anisotropy of traction forces. In addition, this alignment signal may have propagated to cells located at the center in due course of time. The fluorescence actin staining of patterned C2C12 cells followed by orientation distribution analysis also supports the alignment of cytoskeletal actin due to the micropatterning process. The study promotes the application of a simple micropatterning technique as a useful tool to regulate the orientation and behavior of skeletal muscle cells. Thus, the micropatterning strategy developed could be applied to selectively pattern and culture different adherent cell types, which could prove to be a useful platform for the exploration of various cellular dynamics, including proliferation and signaling.